Pergamon

Journal of Structural Geology, Vol. 20, No. 12, pp. 1625 to 1640, 1998

0191-8141/98/$ - see front matter

PII: S0191-8141(98)00054-6

Fault-valve behaviour in optimally oriented shear zones: an example at the Revenge gold mine, Kambalda, Western Australia

PHUNG T. NGUYEN*

Tectonics Special Research Centre, Department of Geology and Geophysics, The University of Western Australia, Nedlands, WA 6907, Australia

STEPHEN F. COX†

Geology Department, The University of Newcastle, Callaghan, NSW 2308, Australia

and

LYAL B. HARRIS and CHRIS McA. POWELL

Tectonics Special Research Centre, Department of Geology and Geophysics, The University of Western Australia, Nedlands, WA 6907, Australia

(*Received* 1 *July* 1997; *accepted in revised form* 27 *May* 1998)

Abstract—Quartz vein systems developed in and adjacent to shear zones host major gold deposits in the Kambalda region of the Norseman–Wiluna greenstone belt. At the Revenge Mine, two groups of mineralised reverse shear zones formed as conjugate, near-optimally oriented sets during ESE subhorizontal shortening adjacent to a major transpressional shear system. The shear zones developed at temperatures of about 400°C in a transitional brittle–ductile regime. Deformation was associated with high fluid fluxes and involved fault-valve behaviour at transiently near-lithostatic fluid pressures. During progressive evolution of the shear system, early brittle and ductile deformation was overprinted by predominantly brittle deformation. Brittle shear failure was associated with fault dilation and the formation of fault-fill veins, particularly at fault bends and jogs. A transition from predominantly brittle shear failure to combined shear along faults and extension failure adjacent to faults occurred late during shear zone evolution and is interpreted as a response to a progressive decrease in maximum shear stress and a decrease in effective stresses. The formation of subhorizontal stylolites, locally subvertical extension veins and minor normal faults in association with thrust faulting, indicates episodic or transient reorientation of the near-field maximum principal stress from a subhorizontal to a near-vertical attitude during some fault-valve cycles. Local stress re-orientation is interpreted as resulting from near-total shear stress release and overshoot during some rupture events. Previously described fault-valve systems have formed predominantly in severely misoriented faults. The shear systems at Revenge Mine indicate that fault-valve action, and associated fluctuations in shear stress and fluid pressure, can influence the mechanical behaviour of optimally-oriented faults.

INTRODUCTION

Vein-type gold deposits associated with shear zone systems have been described as the most important types of gold lode resource in the Archaean Abitibi Greenstone Belt (Kerrich and Allison, 1978; Robert and Brown, 1986; Poulsen and Robert, 1989), in the Yilgarn Craton (Eisenlohr *et al*., 1989), and in the Lachlan Fold Belt (Cox *et al*., 1991), and they account for a large proportion of global gold production. An important aspect of the formation of many of these shear systems is that repeated slip, permeability enhancement and fluid flow associated with mineralisation was controlled by fluctuation in fluid pressure and shear stress (Sibson, 1989; Sibson *et al*., 1988; Cox *et al*., 1991; Boullier and Robert, 1992; Robert *et al*., 1995; Cox, 1995). In deformed terranes, these systems provide insights about timing and localisation of high fluid fluxes during deformation (Kerrich, 1986; Cox *et al*., 1987; Cox, 1995; Robert *et al*., 1995).

Kambalda is one of the largest mining centres in the Norseman–Wiluna greenstone belt of the Yilgarn Craton. The area contains a large number of gold and nickel deposits associated with Archaean metavolcanic and metasedimentary rocks. Major gold production began in Kambalda in 1982 and, to June 1996, 100 tonnes of gold have been produced from more than 10 gold mines, with a resource of a further 200 tonnes of gold defined. As for many other gold deposits in the Norseman–Wiluna Belt, the Kambalda gold deposits are mainly shear zone/quartz vein-hosted, and are localised within low displacement reverse shear zones. The latter have strike lengths up to about 1000 m and maximum displacements up to several tens of metres. These mineralised shear zones are developed adjacent to much larger, kinematically-related NNW-trending regional shear zones (Eisenlohr *et al*., 1989; Roberts

*Current address: WMC Exploration, WMC Resources Ltd, 191 Great Eastern Hwy, Belmont, WA 6984, Australia

†Now at: Research School of Earth Sciences and Department of Geology, The Australian National University, Canberra, ACT 0200, Australia, e-mail:sfcox@geology.anu.edu.au

and Elias, 1990; Nguyen *et al.*, 1992; Nguyen and Donaldson, 1995).

The Revenge gold deposit is a recently developed mine (1991), located 13 km southeast of Kambalda, Australia. Revenge has good three-dimensional exposures in both open pit and underground development to a depth of 300 m. The exposures reveal a shear zone/quartz vein system similar to many mesothermal gold deposits worldwide (Hodgson, 1989; Poulsen and Robert, 1989; Cox, 1995; Robert *et al.*, 1995). Although there are many shear zone-hosted gold deposits in the Kambalda region, limited research has been carried out on the geometry of the shear zones/quartz vein systems and the processes involved their formation. In this paper, the coupling between mechanical behaviour and fluid activity during the formation of mineralised shear zones at Revenge is examined. In particular, the evolution of deformation processes in the shear systems are interpreted in terms of progressive evolution of fluid pressure and shear stress regimes in the gold-producing hydrothermal system.

GEOLOGICAL SETTING OF THE REVENGE DEPOSIT

The Revenge gold deposit is located in the southern part of the Norseman–Wiluna greenstone belt within the Eastern Goldfields Province of the Yilgarn Craton, Western Australia. The Norseman–Wiluna Belt is dominated by volcanosedimentary assemblages with ages of approximately 2.7 Ga (Barley *et al.*, 1990). The belt hosts over two thirds of Australia's known Archaean gold endowment (Woodall, 1990), with the broad distribution of major gold deposits being controlled largely by NNW-trending transcrustal fault systems such as the Boulder–Lefroy fault (Eisenlohr *et al.*, 1989).

The Kambalda area consists of a corridor of predominantly mafic–ultramafic lava and intrusives which have been metamorphosed to grades ranging from upper greenschist facies to lower amphibolite facies (Binns *et al.*, 1976; Archibald, 1985; Wong, 1986; Clark *et al.*, 1989). The area is bounded by two major NNW-trending regional structures: the Boulder–

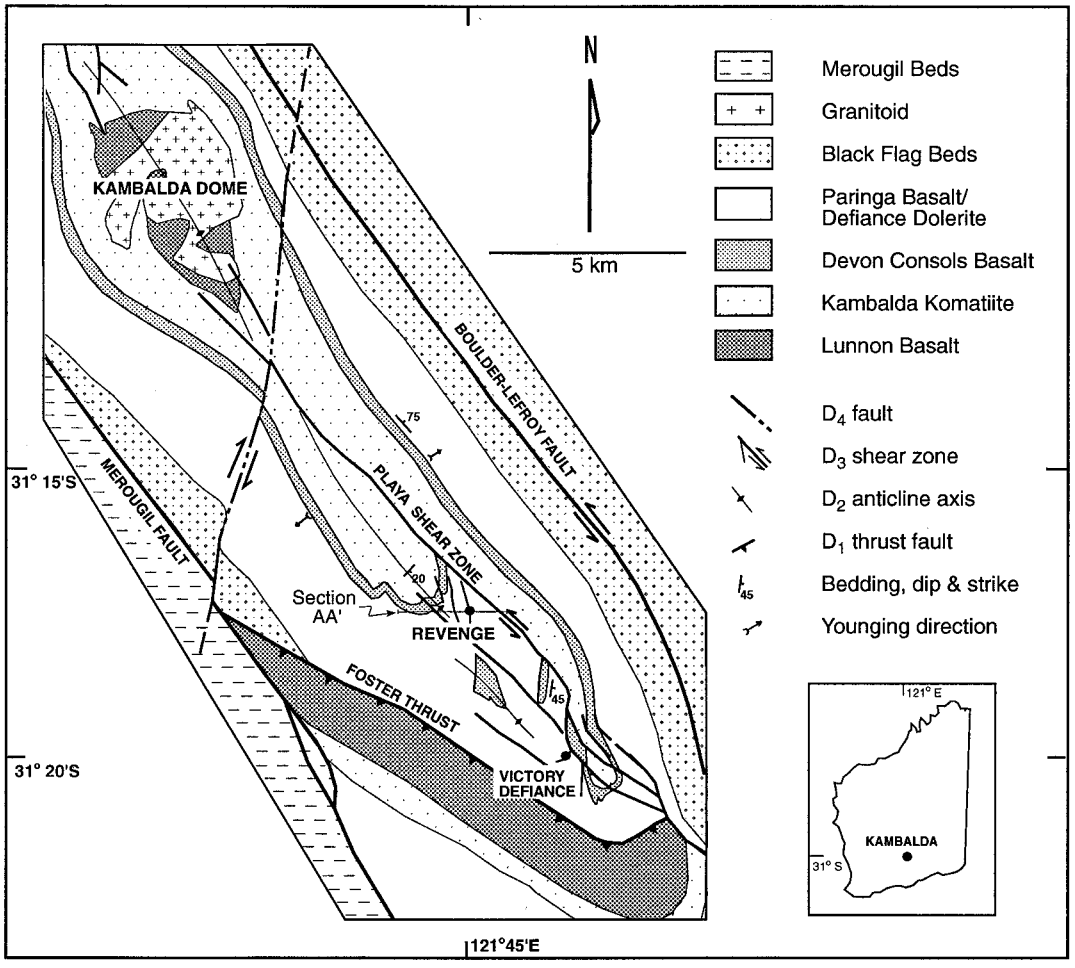

Fig. 1. Solid geology of the Kambalda region, Western Australia, compiled from WMC Resources Ltd surface mapping, drilling data and geophysical data.

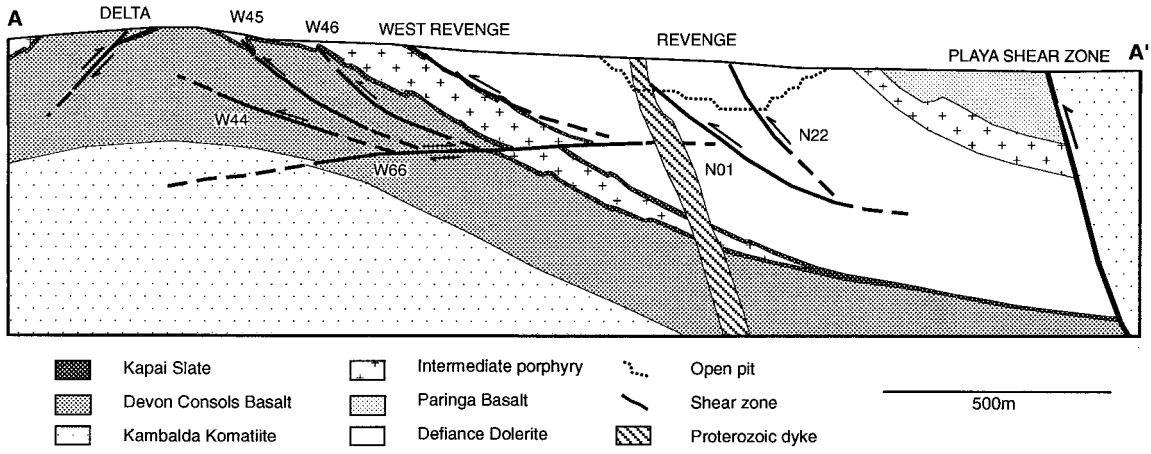

Fig. 2. East–west cross section through the Revenge mine area, showing location of mineralised shear zones.

Lefroy fault to the east and the Merougil fault to the west (Fig. 1) and has undergone four main episodes of Archaean deformation (Nguyen *et al.*, 1995). The first, D_1 produced regional south-over-north thrusts (e.g. Foster thrust, in Fig. 1). The second, D_2, produced upright, NNW-trending, gently plunging folds. The third event, D_3, generated a brittle–ductile, NNW-trending, oblique-sinistral wrench fault system which localised the development of N-trending gold-bearing shear zones. Local N-trending, en échelon, inclined folds are observed close to the D_3 shear zones in some areas and are interpreted to have formed in association with the sinistral wrench system. They are similar to those described as F_3 folds in the New Celebration–Kalgoorlie areas by Swager *et al.* (1990a). The fourth event, D_4, involved the formation of NE-trending dextral faults and dextral $\pm$ reverse reactivation of early structures. Alteration assemblages associated with the gold mineralised shear zones indicate that these structures formed at temperatures of approximately 400°C (Clark *et al.*, 1989). Geochronologic constraints indicate that the mineralised shear systems developed at about 2630 Ma (Clark *et al.*, 1989; Nguyen, 1997).

The Revenge deposit consists of several mineralised structures developed mainly on the eastern limb of a D_2 anticline (Fig. 2). The Kambalda Komatiite is the oldest stratigraphic unit in the Revenge area and has been intersected in several drill holes to the northwest of the Revenge mine. It is overlain by the Devon Consols Basalt, Kapai Slate, Defiance Dolerite and Paringa Basalt. Minor intermediate intrusions (xenolithic diorite) commonly intrude the 10–30 m thick Kapai Slate and other units from the Kambalda Komatiite to the Paringa Basalt. They are syn- to late D_2 lamprophyric rocks (Perring, 1988), which occur as sills to up 70 m thick within the Kapai Slate and the Paringa Basalt, or as narrower plugs in the Devon Consols Basalt and the Defiance Dolerite. Felsic intrusions include early D_3 upright, WNW-trending quartz–albite porphyry dykes, which are exposed throughout the mine area. They vary in thickness from 1 to 10 m and have strike lengths from 10 m to 1 km in the mine area. The Defiance Dolerite is the most important host to the main Revenge structures (N01/S01, N22 lodes). Smaller structures are hosted by the Devon Consols Basalt (Delta, W45, W46, W66 lodes), Kapai Slate (Delta, West Revenge lodes) and Paringa Basalt (S01 lodes). The area is bounded to the east by the steeply (70–80°) NE-dipping Playa shear zone, which separates the Kambalda Komatiite in the hanging wall from younger units in the footwall.

SHEAR ZONE SYSTEM

A complex system of shear zones associated with the third deformation event is recognised in the Revenge area. Two main types of shear zones can be distinguished: (i) NW-trending, sub-vertical, first- and second-order regional shear zones and (ii) smaller, more localised E- and W-dipping mineralised shear zones.

The first-order shear zones, such as the Boulder–Lefroy fault, are from about 10 to 100 m wide and extend up to 200 km along strike. Poor exposures of the Boulder–Lefroy fault to the north and northeast of the Kambalda dome show a NW-trending, subvertical, strongly foliated fabric. Oblique-sinistral movements have been recognised by Mueller *et al.*, (1988), Swager (1989, 1991), Witt (1990) and Swager *et al.*, (1990a,b) for early displacement along Boulder–Lefroy fault. The Playa shear zone has been recognised as a second-order NW-trending shear zone that splays from the Boulder–Lefroy fault system (Nguyen *et al.*, 1992). It is located on the eastern side of the Revenge deposit, and extends for about 10 to 15 km south of the Kambalda dome (Fig. 1). The Playa shear zone is exposed in the 196N01-North airleg drive of the

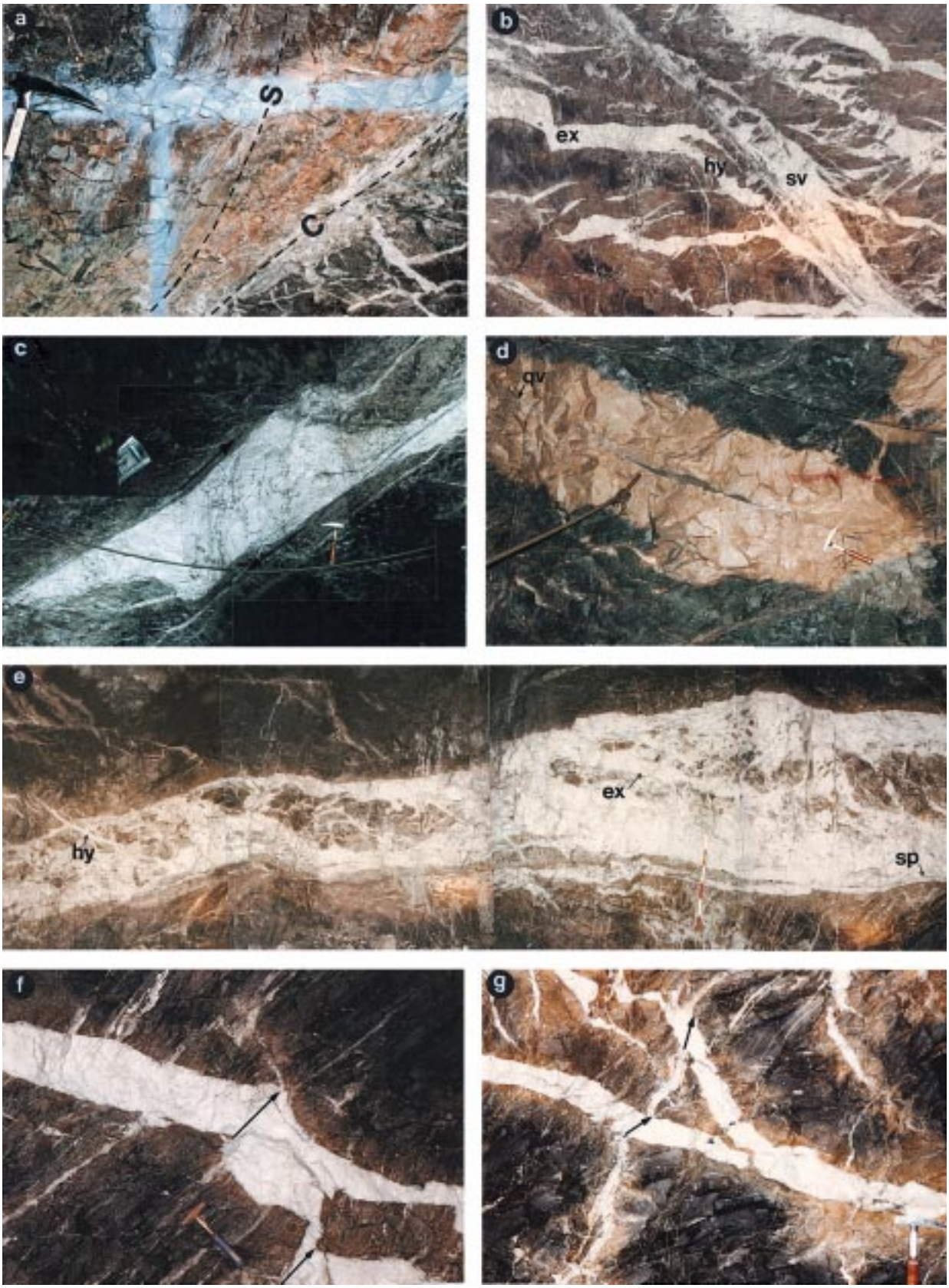

Fig. 3. (a) East-dipping shear zone showing the steeply-dipping foliation (*S*-fabric rotated into a strongly foliated E-dipping *C*-fabric at the principal slip surface); 31 cm hammer for scale. Location S01, 196 S level, looking south. (b) E-dipping shear zone with shear veins (sv), extensional veins (ex) and hybrid veins (hy). Location W45, 200N level, looking north, width of photograph 7 m. (c) Dilational jog in E-dipping N01 shear vein. Location N01, 570N rise, looking south, 31 cm hammer for scale. (d) Unusually thick massive alteration associated with thin quartz veins at the northern end of the N01 shear zone. Location N01-196N, looking east, 31 cm hammer for scale. (e) W-dipping shear zone with

Revenge mine (about 90 m below Lake Lefroy), with Defiance Dolerite in the footwall and strongly foliated Kambalda Komatiite in the hanging wall (Fig. 2). *S–C* fabrics and a moderately SE-plunging stretching lineation in this locally steep NE-dipping shear zone indicate dominantly sinistral-reverse movement.

The two sets of mineralised shear zones in the Revenge mine area are NNW- to NNE-trending, moderately E-dipping (45°) and N- to ENE-trending, gently W- to NW-dipping (15°). Complex quartz vein networks are associated with each of the mineralised shear zones (Figs 3 & 4). Vein types associated with mineralisation are classified as shear veins (or fault-fill veins), extension veins, or hybrid extensional shear veins on the basis of orientation of the veins, dihedral angles between conjugate vein sets, internal structures and opening vectors relative to the vein walls. This classification of vein types is similar to that of Hodgson (1989), Poulsen and Robert (1989) and Sibson (1990). Hybrid extensional shear veins are interpreted to have formed in an extensional shear failure mode (Etheridge, 1983; Hancock, 1985) at moderate stress differences ($\sigma_1-\sigma_3 = 4\,T$ to $6\,T$, where σ_1, σ_3 = maximum and minimum principal stresses, respectively, T = tensile strength of the rocks). They occur as conjugate sets with the acute dihedral angle 2θ typically up to about 45°. Similar veins or fractures have been described as transitional tensile fractures by Suppe (1985), and as oblique-extensional veins (Poulsen and Robert, 1989).

East-dipping mineralised shear zones

The E-dipping shear zones vary in strike from NNW to NNE. The N01/S01 lode is the most important mineralised shear zone in the Revenge area, with high-grade gold mineralisation hosted by the Defiance Dolerite in alteration envelopes immediately adjacent to this structure. The N01/S01 lode comprises northern (N01) and southern (S01) mined sections. The E-dipping shear zones vary from 200 to 1000 m in strike length, extend from 200 to 500 m down dip and range from 0.5 to 12 m in width. Figure 5 shows a typical E–W cross-section of an E-dipping shear zone associated with a localised N- to NNE-trending, subvertical to steeply (80–90°) W-dipping foliation. This foliation (*S*-fabric) progressively rotates towards parallelism with a strongly foliated, E-dipping shear fabric (*C*-fabric) near the slip surfaces in the centre of the shear zone (Figs 5 & 3a). A mineral elongation lineation and slickenfibres defined by biotite–chlorite are well-developed on N01/S01 shear surfaces and pitch from 85°N to 80°S. The metadolerite-hosted alteration assemblages developed in and adjacent to the shear zones comprise an outer envelope of chlorite–carbonate near the margin of the shear zone, grading into a strongly foliated chlorite–biotite zone, which encloses an albite–carbonate–quartz–pyrite zone near the centre of the shear zone and immediately adjacent to the associated quartz veins. The orientations of lineations and sense of curvature of shear zone foliation in the E-dipping shear zones (Fig. 5) indicate that they are reverse shear zones, which formed by ESE subhorizontal shortening and subvertical extension.

As the shear zone foliation is defined by undeformed, but highly-oriented biotite and chlorite, together with elongate aggregates of other minerals (carbonate, quartz, albite) produced during hydrothermal alteration, the foliation is interpreted to have formed during hydrothermal alteration. However, the presence of undeformed carbonate poikiloblasts and randomly oriented biotite overprinting foliation within the shear zones indicates that some hydrothermal alteration outlasted the formation of the shear zone foliation.

Complex quartz vein systems consisting of shear veins, extensional veins and rare hybrid veins are also associated with the E-dipping shear zones. *Shear veins*, which are 5–70 cm thick and 10–100 m in strike length at the centre of the shear zones, are characterised by both laminated and brecciated textures (Fig. 3b). Dilational jogs are present where the shear veins change to more gentle dip, or where en échelon shear veins have linked (Fig. 3c). Breccia veins generally contain small (1–10 cm), and typically unfoliated wallrock fragments, which are cemented by vein carbonate and quartz. *Extensional veins*, which are N- to NE-trending and subhorizontal to gently (5–25°) E-dipping, occur as single veins or as groups throughout the shear zones, and are most abundant in felsic host rocks. The extensional veins vary in thickness from 1 to 30 cm and can extend for up to 20 m from the centre of the shear zones. They commonly cut the shear veins and have a visible albite–carbonate–pyrite alteration halo. *Hybrid veins* are commonly present as both subhorizontal and moderately E-dipping (40–50°) linking segments between gently (10–25°) E-dipping pure extensional veins. The intensity of veining commonly diminishes toward both the northern and southern ends of the shear zones, where the latter taper into

large breccia-containing shear vein occupying a subhorizontal dilational jog. Near the margin, laminated textures defined by slivers of wallrocks taper into thin layers of sulphide (sp). A gently E-dipping extensional vein (ex) and steeper hybrid veins (hy) cut the breccia vein. Subvertical foliation with carbonate–biotite–albite foliae is well defined in the footwall and rotated into a gently W-dipping fabric near the shear vein. Location W66, 104W level, looking north, scale bar 1.2 m. (f) Extensional vein with an opening direction at a high angle to the vein wall, as indicated by net displacement of irregularities in the vein wall. Location W66, 104E level, looking north, 31 cm hammer for scale. (g) Hybrid veins with opening directions at a high angle to the vein walls. Note the rotation of the foliation near the steeper vein, indicating shearing during formation of the vein. Location W66, 115W level, looking north, 31 cm hammer for scale.

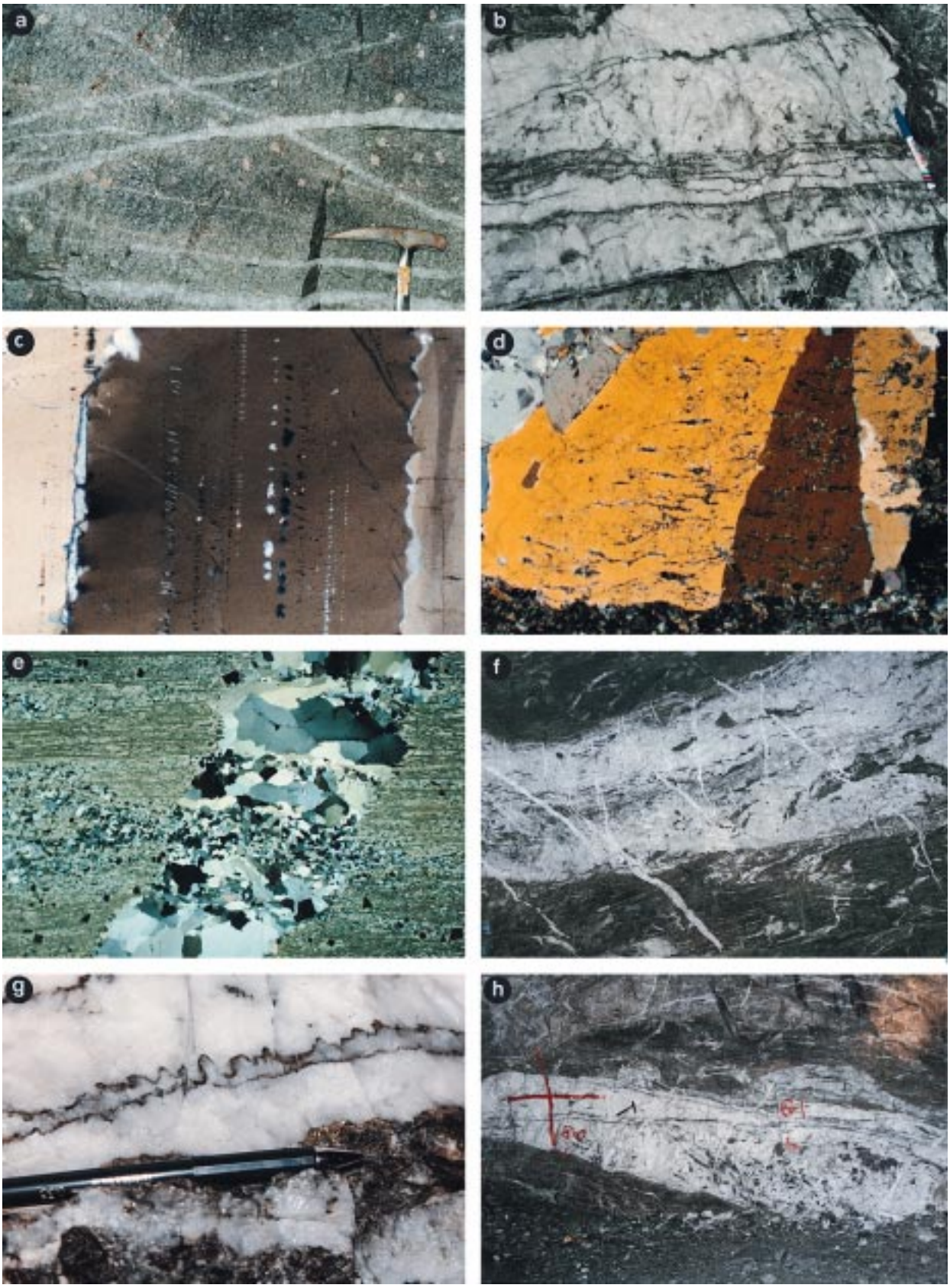

Fig. 4. (a) Hybrid vein set in felsic porphyry. Location W66, 110W level, looking south, 31 cm hammer for scale. (b) Laminated shear vein with layers of sulphide and wallrock material. Note the laminated vein truncates a breccia vein in the lower portion of the photo and a late fault cuts the laminated vein in the upper right corner. Location W66, 110W level, looking north. (c) Photomicrograph in cross nicols of albite inclusion trails in quartz crystals. Section Z61268, width of photo 0.5 mm. (d) Photomicrograph in cross nicols of gently undulating albite- and carbonate-bearing inclusion bands in subhorizontal quartz extension vein. Elongate quartz grew antitaxially from the albite–carbonate-altered host

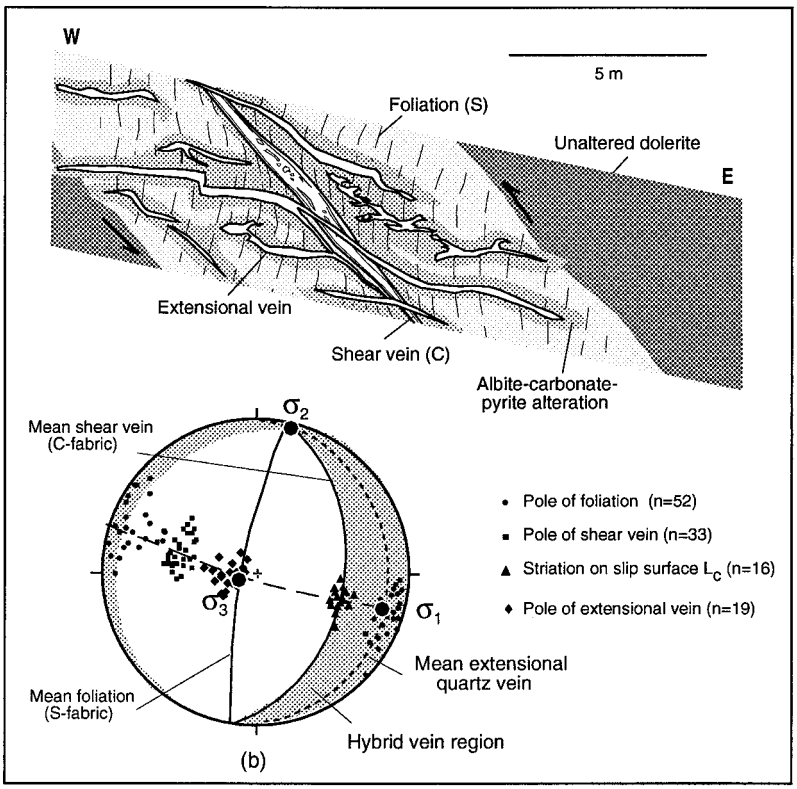

Fig. 5. Schematic diagram showing a typical E–W cross section of the N01 shear zone with structural data presented on an equal-area lower hemisphere stereoplot.

narrow (20–50 cm) foliated zones. At the northern ends of the N01/S01 and W45 lodes, unusually thick (0.5–1.0 m) massive albite–carbonate–pyrite alteration is associated with very thin (1–5 mm) extensional quartz veins developed at the margins of the shear zones (Fig. 3d).

West-dipping mineralised shear zones

The W-dipping shear zones comprise the main W66 shear zone and a smaller shear zone (CO2) to the west. The W66 shear is located at a depth of between 200 and 300 m below the current surface level and extends for more than 300 m in both strike length and down dip; it ranges in thickness from 1 to 10 m. This shear zone is hosted principally by the Devon Consols Basalt, but it extends eastward into the Kapai Slate and dioritic prophyry. Towards the northwest, the shear zone intersects the Kambalda Komatiite, where it thickens and has lower gold grades. Mining and drilling to date have not yet defined the total extent of the W66 shear.

The W66 shear zone is a subhorizontal to gently W- to NNW-dipping (10–15°) curved surface, that comprises undulating zones of intensely foliated rocks and a core of thick (from 0.1 to 5.0 m) fault-fill veins (Figs 3e & 6). The strike of the shear zone ranges from 040° to 080° in the eastern section of the shear zone and between 350° to 010° in the western section of the shear zone, but with some local variations. On the basis of shear sense indicators (veins and rotated foliation) and stratigraphic separations of the dioritic porphyry and the Kapai Slate, the maximum displacement along the shear zone is about 70 m of reverse slip. Smaller (0.2–1 m thick) shear zones which splay off the main shear are common, especially where the main shear intersects different host rocks or changes its orientation. The splays have limited dip and strike extent (less then 50 m) and have steeper (30–50° W) dips than the main shear. As in the E-dipping shear zones, the shear zone foliation is NNE-trending and

rock in the lower section of the photo. Section Z64156, width of photo 5.6 mm. (e) Photomicrograph in cross nicols of a hybrid vein with elongate quartz at a high angle (70°) to the vein wall. Note the zones of small quartz grains between coarser, more deformed elongate quartz. The zones of fine-grained quartz appear to be aligned with quartz-rich domains in the intensely foliated biotite–abite–quartz wallrock. Section Z61220Z, width of photo 30 mm. (f) Large subhorizontal shear vein with several narrow vertical dilational quartz veins and late E-dipping hybrid veins. Note the mutually overprinting relationship between the vertical dilational veins and the shear vein. Location W66, 134E level, width of photograph 6 m, looking north. (g) Stylolitic textures developed in the sulphide layers of subhorizontal shear veins. Location W66, 110W level, looking south. (h) Shear vein with several sulphide layers developed across the vein. The large brecciated zone in the lower section of the vein is interpreted to have developed at a dilational bend in the shear zone. Location W66, 115W level, 31 cm hammer for scale, looking north.

steeply (80–90°) west-dipping near the shear zone boundary, but rotates towards parallelism with the shear surfaces near the centre of the shear zone (Figs 3e & 6). Mineral elongation lineations and slickenfibres on *S*- and *C*-surfaces pitch between 70° and 90° NW. The plunge direction of the lineation varies from WNW to NW in accordance with the strike variation of the foliation. This variation could reflect a NW-trending, very gentle fold of the shear, perhaps associated with the D_4 dextral reactivation on the large regional shear zones. Geometrical relationships and kinematic indictors, such as displacements of rock units, rotation of foliation and *S–C* fabrics, all indicate that the W66 is a thrust zone, and indicate approximately ESE sub-horizontal shortening and subvertical extension at the time of formation.

Vein development in the W66 shear zone includes large (0.1–5 m wide) shear veins and narrow (1–10 cm) extensional and hybrid veins (Fig. 3e–g) filled predominantly by quartz and subordinate carbonate and albite. *Shear veins* are particularly well developed in the W66 shear zone where they typically occupy its core and are sub-parallel to shear zone boundaries. Toward their ends, shear veins taper into narrow zones of foliated host-rocks.

Extensional veins in the W66 shear zone are less well-developed than in the E-dipping shear zones. They are narrow (1–20 cm wide), vary in strike from 005 to 040° and dip from 10 to 30° to the east; they commonly occur as single veins cross-cutting larger shear veins and extend for up to 3–10 m away from the shear zone core. Extension veins with sub-planar boundaries form both perpendicular and oblique to the shear zone foliation; their opening vectors (approximately perpendicular to the vein wall) can be determined using the displacement of wallrock fabric and vein wall irregularities (Fig. 3f). *Hybrid veins* form as groups of irregular to planar thin veins (10–50 mm wide) at a high angle to the subvertical foliation. These veins occupy conjugate dilational shear fractures, which trend NNW to NNE and dip either subhorizontally or 30–40° E (Fig. 3g). The acute dihedral angle (2θ) between the conjugate sets is thus typically around 30–40°. Mutually cross-cutting relationships between the east- and west-dipping conjugate hybrid veins indicate that they formed contemporaneously. Most extensional and hybrid veins cut the shear veins and have prominent albite-rich alteration halos. The hybrid veins are best developed in the felsic and intermediate porphyries (Fig. 4a) and in the more steeply-dipping, thinner segments of shear veins.

INTERNAL TEXTURES OF THE VEINS

The internal structures of gold-bearing quartz veins provide a record of displacement, stress regimes and fluid pressure history during the development of shear zone/quartz vein systems (Robert and Brown, 1986; Cox *et al.*, 1987; Hodgson, 1989; Poulsen and Robert, 1989; Boullier and Robert, 1992; Vearncombe, 1993; Cox, 1995; Robert *et al.*, 1995). Although shear veins are well developed in the W-dipping shear zones and extension veins are more common in the E-dipping shear zones, similar internal structures are observed for both E- and W-dipping shear zones.

Shear veins

The dilational, fault-fill veins display a variety of internal textures ranging from uniform, massive quartz to complex internal structures in which the total vein width may include a number of texturally distinct zones. For example, in the W66 shear zone, fault-fill veins are locally coarsely banded due to the presence of several zones of laminated quartz, massive quartz and breccia veins in the one section. Where developed, individual textural zones are sub-parallel to the shear vein boundaries, up to several tens of centimetres thick, and continuous for about 50–100 m along both dip and strike.

Breccia veins are more common in the W66 shear zone than in the E-dipping shears and comprise two main types: coarse breccia and microbreccia. Development of thick zones of *coarse breccia* in shear veins is commonly localised in dilational jogs on the releasing side of the curved shear surfaces (Fig. 6). The coarse breccia veins consist of large (10–50 cm in diameter), commonly unfoliated, angular wallrock fragments and usually occupy the central region of the shear veins (Figs 3e & 4h). The wallrock fragments generally do not contact each other and are cemented by early crustiform, comb-textured to euhedral albite,

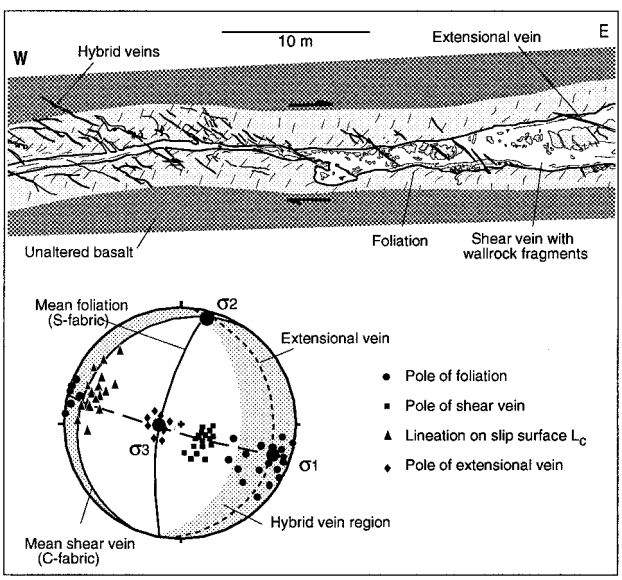

Fig. 6. Schematic diagram based on mosaic photographs of an E–W cross-section of part of the W66 shear zone. Orientation data are presented on an equal-area lower hemisphere stereoplot.

quartz and carbonate, and by later anhedral quartz and subordinate carbonate and albite. The fragments are partly or wholly altered and replaced by hydrothermal minerals such as albite, biotite and calcite. The coarse breccia zones appear to have formed by incremental dilation of the shear zones, particularly at dilatant jogs or bends. Much finer-grained microbreccia occurs locally as thin sub-planar bands which are parallel to, and commonly near the footwall margin of shear veins, especially in the W66 structure. The microbreccias contain small (1.0–10.0 mm) fragments of both foliated wallrocks and early feldspar–carbonate infill. The matrix between clasts is mainly quartz with a dense network of dilational microfractures. The closed framework textures of the microbreccias contrast with the open framework textures of the coarse breccias. The geometry and textures of the microbreccia bands indicate that they are probably cataclasites produced during fault slip at the margins of shear veins.

Laminated veins commonly occur at the margins of thinner shear veins (Fig. 4b) and typically contain several thin (0.1–10 cm) slivers of wallrock tapering into thin layers (0.1–3.0 mm) of sulphide. The sulphide layers are composed mainly of pyrite, subordinate wallrock materials and free gold. In thin section, laminated shear veins comprise multi-layers of fine-grained quartz, which are separated by thin layers of sulphide and fine-grained wallrock materials (biotite, albite, carbonate, muscovite, chlorite). The original microstructures of fine laminated veins (spacing < 5 mm) are rarely preserved owing to intense shearing. Quartz, carbonate and albite are usually plastically deformed and partly recrystallised. Significant differences in grain size between quartz lamina are observed, with quartz grains commonly showing lobate, bulged grain boundaries and intense undulose extinction.

Buck quartz veins are typically between 10 and 50 cm thick and contain milky white massive quartz with a grain-size up to 3 cm. They are most common near the centre of shear veins and between breccia veins. The coarse quartz occurs as weakly deformed anhedral to euhedral grains associated with less abundant albite and carbonate. These massive textured veins locally cut across the laminated veins and the breccia veins.

Pure extensional- and hybrid extensional-shear veins

Extensional veins exhibit a variety of textures, ranging from fibrous to massive textures formed by crack–seal processes, to massive to crustiform textures produced by continuous growth processes in open fractures.

Elongate to fibrous vein textures consisting of straight or slightly curved quartz, feldspar and carbonate crystals subperpendicular to the wall are common in small extensional veins (0.5–2.0 cm). Evidence for *crack–seal* growth processes is common in antitaxial veins, where trails and bands of small (2–10 μm) inclusions of albite and carbonate occur within quartz crystals (Fig. 4c). The inclusion bands can be straight or gently undulating parallel to the vein margins (Fig. 4d), with spacing between inclusion bands varying from 50 to 200 μm. Another crack–seal texture is the characteristic saw-tooth boundary between fibres, which is similar to that described by Ramsay (1980) and Cox *et al*. (1987) for vein quartz that has undergone repeated intragranular fracturing and sealing.

Open-space filling textures produced by continuous growth, rather than episodic crack–seal processes, are common in large massive extensional veins, which are filled by euhedral crystals attached to the vein wall. The infill minerals comprise dominantly quartz and subordinate calcite, albite, muscovite, pyrite, chlorite, scheelite and free gold.

Hybrid veins have textures similar to the pure extensional veins, with quartz and minor carbonate and albite forming elongate grains with long axes at moderate to high angles (50–80°) to the vein wall. Figure 4(e) shows a hybrid quartz vein with zones of fine-grained quartz between weakly deformed (undulose extinction and serrated grain boundaries) coarser quartz. Here, the zones of fine-grained vein quartz have formed adjacent to fine-grained quartz-rich domains in the intensely foliated wall rock. The texture of the fine-grained zones in the veins is interpreted to have been influenced at least partly by an epitaxial growth relationship with the fine quartz at the vein margin. However, the microstructure may also have been influenced by localised deformation and recrystallisation of quartz.

In places, carbonate is replaced by quartz or albite. Other textures such as undulose extinction, sutured grain boundaries, stylolites and bent crystals indicate mild deformation in extensional veins. Uncommon early-formed and gently buckled to ptygmatically folded veins exhibit more pronounced overprinting of primary vein textures by plastic and brittle deformation.

Timing relationships between vein types

Within the shear zones, coarse dilational breccia veins containing unfoliated fragments appear to have formed earlier than the thinner and more regular bands of cataclastic microbreccias which contain intensely foliated wallrock fragments. Both types of breccia veins are typically cut by later buck quartz and laminated quartz veins. The massive, buck quartz veins in turn cut across laminated veins. Rare, early extensional veins are usually quite deformed (tightly folded) near the centre of shear zones, and are cut by shear veins. However, most of the extensional veins are late as they

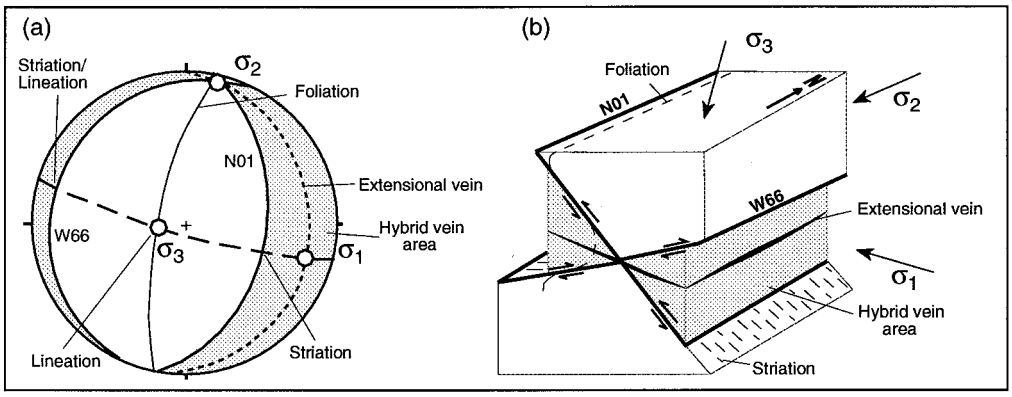

Fig. 7. (a) Interpretation of the principal stress orientations in the Revenge area during formation of the mineralised shear zones, and (b) schematic block diagram showing the relationship between different shear and fracture sets and the stress field.

are relatively undeformed and cut across the various textural zones in shear veins.

OTHER SHEAR-RELATED STRUCTURES

Steeply-dipping quartz veins are common in the centre of the W66 shear zone (Fig. 4f). These veins are narrow (1–10 mm) and of limited areal extent (0.5×1.0 m). They have mutually overprinting relationships with the shear veins: some early veins cut only the brecciated zones and are themselves cut by buck quartz and laminated zones; other later veins cut the laminated zones but are cut by the late extensional and hybrid veins. The cross-cutting relationships indicate that the steeply-dipping quartz veins have formed during the formation of the shear zones.

Stylolites are extensively developed within the fault-fill quartz veins, at both the microscopic and mesoscopic scale (Fig. 4g). These dissolution seams are characterised by local concentration of sulphide and minor chlorite, albite and muscovite. The stylolitic shapes range in type from irregular to peaked with low amplitudes, in which the peaks of the stylolites, and hence maximum principal stress (σ_1), are oriented subvertically. Stylolitic textures are best developed within the sulphide layers in the subhorizontal segments of shear veins, where the stylolitic textures are more symmetrical than those in the more steeply-dipping segments of shear veins. Discrete superposed normal faults are locally present, particularly in the footwall of the shear zones. The faults are subvertical and have limited strike extents (1–2 m), with displacement varying from millimetres to centimetres. Normal slips are easily recognised by separation and rotation of fabrics along the faults. Planes of fluid inclusions in the quartz veins are either subhorizontal (parallel to the subhorizontal vein walls) or subvertical (perpendicular to the vein wall).

DISCUSSION

Shear zone kinematics and vein distribution

Geometric and kinematic data for the E- and W-dipping shear zones and their associated quartz vein systems at Revenge Mine indicate that they are reverse shear zones which probably formed as a conjugate set during ESE subhorizontal shortening and subvertical extension (Fig. 7). These structures are interpreted as small splays from the kinematically-related, NW-trending, sinistral-reverse Playa fault.

The margins of all shear zones are characterised by the development of a NNE-trending, steeply-inclined foliation which increases in intensity as it becomes less-steeply-dipping and rotates towards the shear plane near the centre of each shear zone, consistent with WNW–ESE shortening. The E-dipping shear zones have relatively uniform dips, an associated relatively regular development of the shear veins and a widespread distribution of extensional veins around the shear zones. In contrast, the W-dipping shear zones have more undulose trajectories. This non-planarity led to the development of large, vein-filled zones predominantly at dilatant jogs and bends in the W-dipping shear zones. Gently-dipping extension veins and hybrid extensional-shear veins also have an irregular distribution around several of the shear zones, but tend to be more common near bends and dilational jog segments of the W66 shear.

The proposed sequence of formation of the fault-vein systems in the Revenge area is illustrated in Fig. 8. Some initial brecciation events pre-date the formation of foliation within the shears, and appear to have been localised at broad dilational jogs or fault bends. The subsequent development of laminated and massive quartz veins, which tend to cut across most breccia zones, was also localised along jogs. This is particularly well-illustrated by the extensive area of laminated

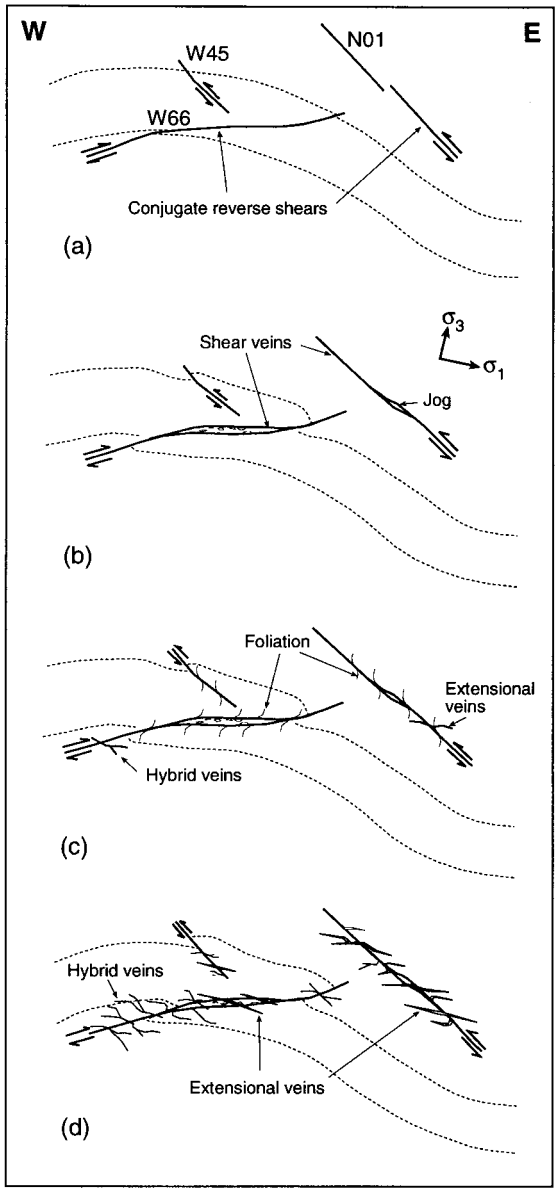

Fig. 8. Proposed sequence of formation of structures in the Revenge shear zone/quartz vein systems. (a) Early brittle shear failure. (b) Shear failure associated with formation of shear veins and dilational breccia. (c) Ductile shearing associated with formation of chlorite–biotite foliation, interspersed with episodes of brittle shear failure and formation of minor hybrid and extensional veins. (d) Main phase of formation of hybrid and extensional veins which crosscut the shear zone foliation. The dashed lines represent the upper and lower boundaries of the Devon Consols Basalt.

fault-fill vein in the more gently-dipping segments of the W66 structure (Fig. 8). Hybrid extensional-shear veins and pure extensional veins typically cross-cut the shear zone foliation and most of the textural zones in fault-fill veins. Accordingly, they are interpreted to have developed predominantly in the later stages of shear zone evolution. However, some thin, early, deformed extension veins are present at the margins of most shears.

Hybrid veins are more common in the wallrock adjacent to the steeper segments of the W66 shear zone, whereas extension veins are common within the less steeply dipping segments of the shear zone where coarse breccias are developed. As the formation of extensional shear fractures requires higher stress differences than for pure extension fractures (Secor, 1965), this spatial variation in vein styles may reflect a local change from higher shear stresses in the steeper fault segments to lower shear stresses in the less-steeply-dipping jog segments during vein growth.

Role of fluids and alteration in the formation of the vein system

Although there are some local variations in timing relationships between different vein types, in general, shear veins appear to have initiated during the early stages of shear zone evolution, whereas hybrid and extensional veins formed predominantly late in the slip history. Early brittle shear failure and breccia formation was followed by a period of more ductile deformation and foliation development within a developing envelope of hydrothermal alteration around the core of the shear zones. Repeated transitions between brittle and ductile shearing during this period, and between the formation of shear failures, hybrid extensional-shear failures and pure extensional failures later during shear zone evolution, require changes in shear stress and effective stress states during progressive deformation of the shear complex.

The evolution of effective stress states associated with failure episodes during formation of shear zones and vein systems at the Revenge mine is illustrated

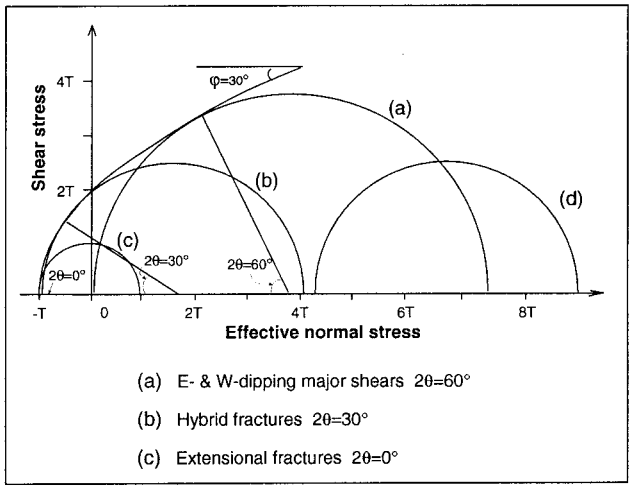

Fig. 9. Mohr diagram representation of stress states during formation of Revenge shear zones and vein systems. The large stress circle (a) represents the stress state for early brittle shear failure which produced the main E- and W-dipping shear zones, shear veins and dilational breccias at relatively high stress differences and high, but sublithostatic fluid pressures; the smaller circles represent stress states for formation of hybrid fractures (b) and pure extension fractures (c) at lower stress differences and supralithostatic fluid pressures. Stress circle (d) represents a potential effective stress state associated with ductile straining at reduced fluid pressures between slip episodes along the shear zones.

qualitatively using Mohr circle constructions in Fig. 9. The earliest breccia-forming events pre-date much of the ductile shearing and accompanying foliation development in the dolerite host-rock, and indicate brittle shear failure at moderate stress differences and high (near-lithostatic) fluid pressures (stress circle 'a'). The near-optimal orientation of the shears with respect to the inferred maximum principal stress orientation does not require supralithostatic fluid pressures. However, the development, within the shear zones, of some short and narrow subhorizontal quartz extension veins which have been strongly deformed during the period of ductile straining of the shear zones, does indicate that fluid pressures were at least transiently greater than the near-field minimum principal stresses during the earliest stages of shear zone evolution (stress circle 'c').

Repeated transitions between brittle shear failure events (and associated formation of shear veins) and ductile shearing (associated with the development of a shear zone foliation adjacent to shear veins) are interpreted in terms of cyclic changes in fluid pressures and shear stresses during progressive shear zone evolution. Brittle shear rupture could only occur when and where fluid pressures were high enough for the stress circle to contact the failure envelope (circle 'a'). Ductile straining along the shear zone is interpreted to have occurred also in response to moderate shear stresses, but at lower fluid pressures and higher effective stresses than 'a' which inhibited brittle shear failure (e.g. stress circle 'd'). If brittle rupture events at this stage of shear zone evolution were fast, possibly seismic slip events, then the ductile shearing could represent aseismic creep between slip episodes, occurring at depths near the base of the seismogenic regime.

The progressive change from mixed brittle and ductile deformation to fully brittle deformation at Revenge is unlikely to be a response to substantially decreasing temperatures during shear zone evolution. Although deformation occurred in a post-peak metamorphic regime and could have been associated with exhumation after D_2 crustal shortening, the hydrothermal alteration assemblages produced during shearing and vein development do not indicate substantial changes in temperatures during progressive deformation. In this case, the progressive evolution from mixed brittle–ductile deformation, early in shear zone evolution, to purely brittle deformation at later stages, is more likely associated with a systematic decrease in effective stresses due to increased fluid pressures as the shear zones matured and localised fluid flow within the large-scale hydrothermal system associated with gold mineralisation in the region.

Similarly, the gradual change from dominantly shear-mode failure to mixed shear-mode and extension-mode failure, and finally to dominantly extension-mode fracture or hybrid extensional shear during the latest stage of shear zone evolution (especially in the W66 structure), is also interpreted to indicate a progressive decrease in shear stress and an increase in fluid pressures (decreased effective normal stresses) during failure events.

The observation that the acute angle between the apparently conjugate shears at Revenge is approximately 60° indicates that the shears are nearly optimally-oriented (Sibson, 1985) with respect to the maximum principal stress direction. On this basis the angle of internal friction in the Defiance dolerite at Revenge is assumed to be 30°. This corresponds to a coefficient of friction of approximately 0.6. This value is at the lower end of the typical range of friction coefficients determined experimentally for common crustal rocks (Byerlee, 1978).

Progressive hydrothermal alteration of wall-rock may also have played a critical role in influencing the progressive mechanical evolution of shear zones at Revenge. The distribution of alteration assemblages around the shear zones and associated vein arrays indicates that the earliest alteration assemblages were biotite–chlorite dominated. So the transition from early breccia-producing brittle slip events to a mixture of episodic slip events and intervening ductile creep, involving the formation of shear zone foliation, is interpreted to be partially a response to reaction-enhanced weakening induced by formation of biotite- and chlorite-rich alteration assemblages. Late proximal alteration involving albite–quartz–carbonate–pyrite-rich assemblages may have promoted late reaction hardening which inhibited ductile creep and fostered a transition to dominantly brittle behaviour late during shear zone evolution.

Fault-valve behaviour

The geometry, timing relationships and microstructures of the quartz veins provide evidence that fault slip, dilation and sealing were cyclically repeated processes characteristic of fault-valve behaviour in high fluid flux fault systems (Sibson *et al.*, 1988; Sibson, 1989; Boullier and Robert, 1992; Cox, 1995; Robert *et al.*, 1995).

Under general fault-valve models, shear failure is interpreted to be triggered when sufficient fluid pressure is built up to overcome the time-dependent fault shear strength. The laminated and layered structures with their textural variations in the fault-fill veins provide clear evidence of episodic slip and fault sealing, especially in the dilatant jog segments of faults. The thin slivers of wallrock and sulphides in fault-fill veins are interpreted to have become detached from the vein wall during slip episodes and trapped as inclusion layers during hydrothermal sealing of dilatant sites by quartz deposition. The sulphide layers have spacings varying from millimetres to metres (Fig. 4b) and provide markers to indicate the opening paths of the veins. Figure 4(h) shows a shear vein with several sul-

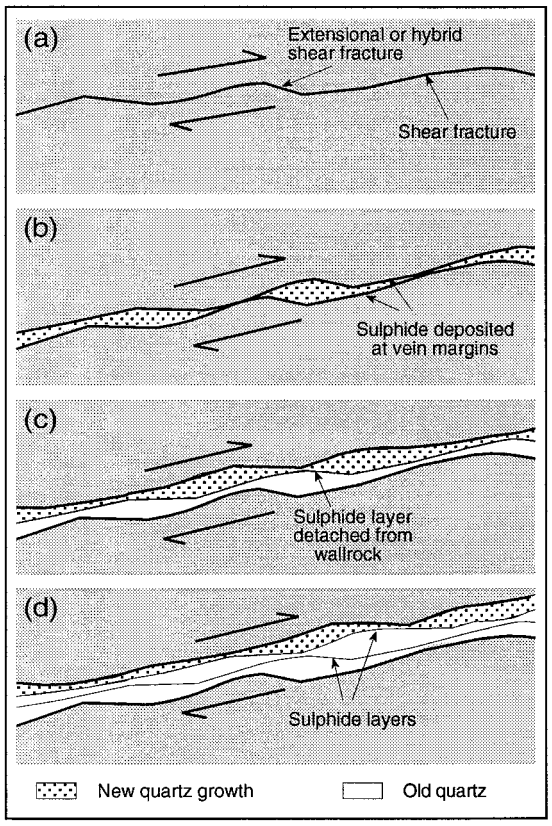

Fig. 10. Schematic diagram showing a thick shear vein (e.g. W66 shear vein) formed by repeated episodes of slip on an undulating fracture in which quartz infilled the dilatant zones on the releasing sides of uneven surfaces after each incremental movement. The displacement associated with each major slip event is indicated by the spacing of the sulphide layers, trapped between old- and new-growth quartz. Modified from Hodgson (1989).

phide layers developed across the vein. This pattern demonstrates that one thick shear vein may have formed by repeated episodes of slip and sealing on an undulating fault surface as schematically illustrated in Fig. 10. The sulphide layers in shear veins provide evidence for meso-scale crack-seal at the early stages of shear zone evolution, whereas the wallrock inclusion bands and inclusion trails in the extensional veins (Fig. 4c & d) may provide a micro-scale version of the process at later stages. Crack-seal textures in extensional veins have been interpreted by Cox (1987, 1995) and Cox *et al.* (1991) as evidence for fluid pressure fluctuations associated with repeated slip events.

The geometries of the shear zones and their quartz vein systems indicate that slip was associated with ESE-subhorizontal shortening and subvertical extension. However, the development of stylolites with subvertical peaks, together with normal faults, narrow subvertical quartz veins and brecciated zones is particularly significant. These structures all indicate that minor subvertical shortening occurred within the shear zones. Mutually overprinting relationships between these structures and those associated with thrusting indicate that minor episodes of subvertical shortening were interspersed with the more predominant subhori-

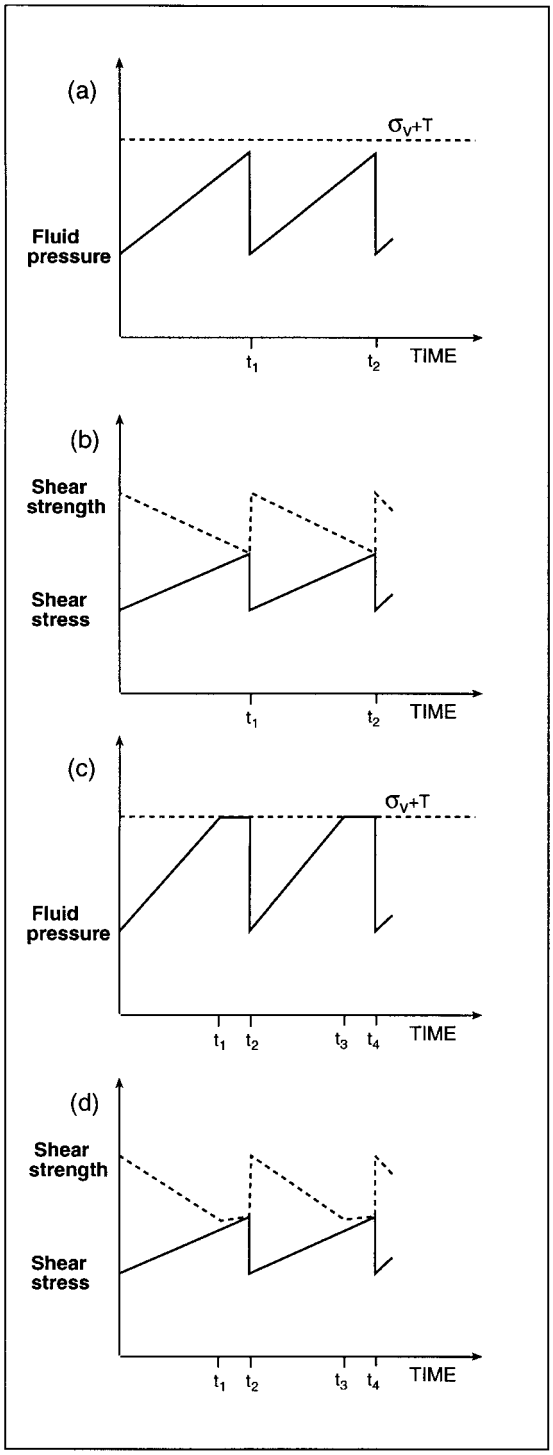

Fig. 11. Schematic illustration of evolution of fluid pressure, shear stress and shear strength with time during fault-valve cycles. (a) Cyclic build-up of fluid pressure prior to rupture events at times t_1 and t_2. Fluid pressures never attain supralithostatic levels. $\sigma_V + T$ is the fluid pressure required to open gently dipping extension hydrofractures. (b) Variations in fault shear strength in response to fluid pressure variations illustrated in (a). Rupture nucleation occurs when decreasing shear strength equals increasing shear stress. (c) Cyclic variations of fluid pressures during fault-valve behaviour where fluid pressures rise to supralithostatic levels and promote opening of extension hydrofractures adjacent to faults at fluid pressures of $\sigma_V + T$. (d) Time-dependence of fault shear strength as a consequence of fluid pressure variations illustrated in (c). Faults are initially load-weakening, but become slightly load-strengthening after maximum fluid pressures are attained.

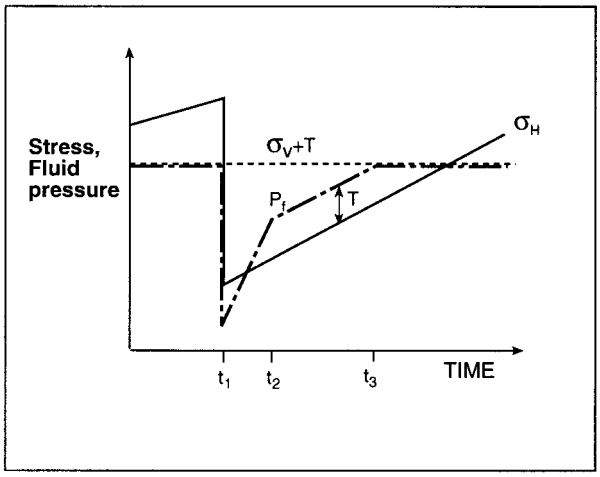

Fig. 12. Schematic illustration of potential variations in fluid pressure (P_f), maximum horizontal stress (σ_H) and vertical stress (σ_V) during fault-valve cycles associated with transient stress reorientation and development of steeply-dipping extension veins together with the more usual gently-dipping extension veins adjacent to shears. Rupture at t_1 is associated with stress relief and a drop in σ_H to values below σ_V. Rapid recovery of fluid pressure allows P_f to exceed $\sigma_H + T$ (where T is the rock tensile strength) at t_2. At this stage vertical extension hydrofractures may open. When σ_H exceeds σ_V at time t_3, fluid pressures attain their maximum value ($\sigma_H + T$). At this stage, vertical hydrofractures close and sub-horizontal fractures may open.

zontal shortening slip events. Transient stress re-orientation of principal stress directions, associated with cyclic changes from horizontal to vertical shortening, have been described previously for reverse faults undergoing fault-valve behaviour by Sibson (1989), Boullier and Robert (1992), Cox (1995) and Robert *et al.* (1995). In their models, transient stress reorientations require near-total shear stress relief during slip events, and may be associated with near-field stress effects or overshoot associated with rupture events.

Fault-valve cycles are considered to be controlled by progressive build-up of fluid pressures between rupture events in fault systems that are the locus of high fluid flux (Sibson *et al.*, 1988; Cox, 1995; Robert *et al.*, 1995). In the Revenge shears, this process is controlled by the migration of high pressure fluids up from deeper levels of the gold-producing hydrothermal system through recently ruptured, and therefore high permeability shears. At the same time, flow in the higher levels of the system is progressively impeded by hydrothermal sealing of fractures between rupture events. In Fig. 11(a), we illustrate what might be a 'typical' fluid pressure cycle during the early brittle deformation history of structures such as the W66 shear at Revenge. In this case, we assume σ_3 ($\approx\sigma_{\text{vertical}}$) remains nearly constant with time. The scarcity of extension vein arrays that have formed in association with the dilational fault-fill (laminated) veins, indicates that in many fault-valve cycles the fluid pressure has not reached levels high enough to induce hydraulic extension fracture (i.e. $P_f > \sigma_3 + T$). Assuming that the shear strength of the faults was controlled by frictional processes (Sibson, 1992), the shears in this case are interpreted to be 'load-weakening' structures (Sibson, 1993) throughout the fault-valve cycle; that is, shear strength progressively decreases with time between slip events due to $\partial P_f/\partial t > \partial\sigma_n/\partial t$, where σ_n = normal stress (Fig. 11b). Shear failure occurs where and when decreased frictional shear strength, due to increasing fluid pressure, equals the progressively increasing shear stress due to shear stress recovery between rupture events. At rupture, opening of jogs and smaller scale asperities, as well as breaching of fault valves, promotes a sudden decrease in fluid pressure. This, together with relief of shear stress due to slip, induces a sudden increase in fault shear strength (Fig. 11b).

In those fault-valve cycles where extension vein arrays have formed adjacent to shears during fault-valve behaviour, we infer that fluid pressures must have been sufficiently supralithostatic (albeit transiently) to induce hydraulic extension fracture. In this case, maximum fluid pressures are limited by the opening of hydrofracture arrays (Cox, 1995) prior to shear failure events (Fig. 11c). The evolution of fluid pressures with time between rupture events may cause the shears to be load-weakening in the early part of the fault-valve cycle, but slightly load-strengthening during the period in which opening hydrofractures limit increases in fluid pressure (Fig. 11d).

The evidence for local and transient stress reorientation indicates that the evolution of stress states and fluid pressures during some fault-valve cycles can be more complex than outlined above. Figure 12 schematically illustrates one scenario in which overshoot or near-field effects such as jog collapse allow the maximum horizontal stress (σ_H) to transiently fall below the value of the vertical stress (σ_V) immediately after rupture. The formation of near-vertical extension veins, such as those present in association with the more usual gently-dipping extension veins in the W66 shear, indicate that after rupture fluid pressures must sometimes have recovered more quickly than σ_H (i.e. $\partial P_f/\partial t > \partial\sigma_H/\partial t$). This can allow fluid pressure to exceed $\sigma_H + T$, and vertical extension veins to form, in the interval before progressive shear stress recovery leads to σ_H again exceeding σ_V (Fig. 12).

High-angle reverse faults, such as those at Sigma Mine, Abitibi (Boullier and Robert, 1992; Robert *et al.*, 1995) and Bendigo-Ballarat, Central Victoria (Cox *et al.*, 1991), have been described as the most typical and efficient fluid-activated 'valves', promoting the largest cyclic fluctuation in fluid pressures (Sibson, 1981). For typical rock friction coefficients (0.6–0.85), slip on such severely misoriented faults (i.e. σ_1 inclined at greater than approximately 60° to fault surface) requires supralithostatic fluid pressures ($P_f > \sigma_3$). In contrast, the Revenge shear zones are very close to optimally oriented as they are inclined at between 25 and 30° to σ_1. For a static coefficient of friction of 0.6, this orientation allows frictional slip along shear fractures at a positive effective stress ratio (σ'_1/σ'_3) of 3.2

and does not necessitate supralithostatic fluid pressures (Sibson, 1985). This type of fault-geometry is similar to that of fault-hosted lode gold deposits at Grass Valley, California (Johnston and Cloos, 1934; Johnston, 1940), where large fault-fill veins are also developed in optimally oriented conjugate faults.

The development of the Revenge shear zones in a gently-dipping and predominantly unfoliated metabasalt sequence has most likely been a key factor allowing the shears to initiate in near-optimal orientations with σ_1 being at a low angle to the gently dipping stratigraphy. Bulk strain in the greenstone sequence during progressive development of the shear zones was insufficient to rotate the shears into unfavourable orientations for reactivation.

CONCLUSIONS

Near-optimally-oriented reverse shear zones with strike lengths up to one kilometre developed at approximately 2630 Ma in the Archaean greenstone sequence in the Revenge mine area, adjacent to a much larger-scale transpressional shear system. These structures formed in a transitional brittle–ductile regime at temperatures around 400°C, near the base of the seismogenic regime. Their formation was associated with localisation of high fluid flux along the shears, the formation of extensive quartz vein systems and associated gold mineralisation and hydrothermal alteration envelopes around the shear zones. The internal structures of the shear zones and associated vein arrays provide evidence that they have evolved by a mixture of aseismic creep and episodic, possibly seismic, slip processes associated with fault-valve behaviour.

Repeated transitions between brittle and plastic behaviour in the early stages of shear zone evolution, and a transition to fully brittle behaviour in the later stages, are interpreted to have been controlled by fluid pressure fluctuations and a progressive evolution of maximum fluid pressures during fault-valve activity. In particular, a transition from predominantly brittle shear failure to late hydraulic extension fracturing in some shears is interpreted to result from decreasing maximum shear stresses and increased fluid pressures during the latest stages of shear zone activity. Episodic and transient reorientation of the principal stresses occurred during shear zone evolution, and is interpreted to have been associated with near-total stress release or overshoot at supralithostatic fluid pressure conditions during some slip events.

This study demonstrates that fault-valve activity may influence the behaviour of optimally oriented shear zones in a transitional brittle–ductile regime. In contrast to severely misoriented faults, these structures can initiate at marginally sublithostatic fluid pressures. Localisation of fluid flow along active shear zones may result in a progressive evolution of the fluid pressure regime and lead to progressive changes in the relative importance of aseismic creep, episodic brittle shear failure and hydraulic extension failure processes during deformation near the base of the seismogenic regime.

Acknowledgements—We thank WMC Resources Limited for financial and logistical support during this study, and for permission to publish these data. The assistance of many WMC geologists and UWA staff, especially R. Watchorn, D. Haynes, N. Hayward, K. Hein, J. Cowan, A. George and S. Wetherley is greatly appreciated. Some of the ideas presented here have been stimulated by discussion with R. Sibson. P.T.N. is supported by an Australian Postgraduate Research Award at The University of Western Australia. A.-M. Boullier, R. Norris and N. Oliver are thanked for review comments. This paper is publication number 23 of the Tectonics Special Research Centre.

REFERENCES

Archibald, N. J. (1985) *The stratigraphy and tectonic-metamorphic history of the Kambalda–Tramway area, WA*. Unpublished WMC Internal Report K/2889.

Barley, M. E., Groves, D. I., Hallberg, J. A., Libby, W. J. and McNaughton, N. J. (1990) Geology and late-Archaean tectonic evolution of the Yilgarn Craton. In *Gold deposits of the Archaean Yilgarn Block, Western Australia: nature, genesis and exploration guides*, eds S. E. Ho, D. I. Groves and J. M. Bennett, pp. 19–29. Geology Department and University Extension, University of Western Australia Publication, **20**.

Binns, R. A., Gunthorpe, R. J. and Groves, D. I. (1976) Metamorphic patterns and development of greenstone belts in the Eastern Yilgarn Block, Western Australia. In *The Early History of the Earth*, ed. B. F. Windley, pp. 303–313. John Wiley and Sons, New York.

Boullier, A. M. and Robert, F. (1992) Palaeoseismic events recorded in Archaean gold–quartz vein networks, Val d'Or, Abitibi, Quebec, Canada. *Journal of Structural Geology* **14,** 161–179.

Byerlee, J. D. (1978) Friction of rock. *Pure and Applied Geophysics* **116,** 807–839.

Clark, M. E., Carmichael, M. D., Hodgson, C. J. and Fu, M. (1989) Wall-rock alteration, Victory Gold Mine, Kambalda, Western Australia: Processes and P–T–X CO_2 conditions of metasomatism. In *The Geology of Gold Deposits: The Perspective in 1988*, eds R. R. Keays, W. R. H. Ramsay and D. I. Groves, pp. 445–459. Economic Geology Monograph, **6**.

Cox, S. F. (1987) Antitaxial crack-seal vein microstructures and their relationships to displacement paths. *Journal of Structural Geology* **9,** 779–787.

Cox, S. F. (1995) Faulting processes at high fluid pressures: an example of fault-valve behaviour from the Wattle Gully Fault, Victoria, Australia. *Journal of Geophysical Research* **100,** 12,841–12,859.

Cox, S. F., Etheridge, M. A. and Wall, V. J. (1987) The role of fluids in syntectonic mass transport, and localization of metamorphic vein-type ore deposits. *Ore Geology Reviews* **2,** 65–86.

Cox, S. F., Wall, V. J., Etheridge, M. A. and Potter, T. F. (1991) Deformational and metamorphic processes in the formation of mesothermal vein-hosted gold deposits—examples from the Lachlan Fold Belt in Central Victoria, Australia. *Ore Geology Reviews* **6,** 391–423.

Eisenlohr, B. N., Groves, D. I. and Partington, G. A. (1989) Crustal-scale shear zones and their significance to Archaean gold mineralisation in Western Australia. *Mineralium Deposita* **24,** 1–8.

Etheridge, M. A. (1983) Differential stress magnitudes during regional deformation and metamorphism: upper bound imposed by tensile fracturing. *Geology* **11,** 231–234.

Hancock, P. L. (1985) Brittle microtectonics: principles and practice. *Journal of Structural Geology* **7,** 437–457.

Hodgson, C. J. (1989) The structure of shear-related, vein-type gold deposits: a review. *Ore Geology Reviews* **4,** 231–273.

Kerrich, R. (1986) Fluid infiltration into fault zones: chemical, isotopic and mechanical effects. *Pure Applied Geophysics* **124,** 225–268.

Kerrich, R. and Allison, I. (1978) Vein geometry and hydrostatics during Yellowknife mineralisation. *Canadian Journal of Earth Sciences* **15,** 1653–1660.

Johnston, W. D., Jr (1940) The gold quartz vein of Grass Valley, California. *U.S. Geological Survey Professional Paper* **194**.

Johnston, W. D., Jr and Cloos, E. (1934) Structural history of the fracture systems at Grass Valley, California. *Economic Geology* **29,** 39–54.

Mueller, A. G., Harris, L. B. and Lungan, A. (1988) Structural controls of greenstone-hosted gold mineralisation by transcurrent shearing: a new interpretation of the Kalgoorlie mining district, Western Australia. *Ore Geology Reviews* **3,** 359–387.

Nguyen, T. P. (1997) Structural controls on gold mineralisation of the Revenge deposit and its setting in the Lake Lefroy area, Kambalda, Western Australia. Unpublished PhD thesis. The University of Western Australia.

Nguyen, T. P., Goodwin, D., Wilkinson, C. and Withers, J. (1992) *Kambalda gold targeting criteria*, p. TN 6. Unpublished WMC Technical Report, **92-014**.

Nguyen, T. P. and Donaldson, J. A. (1995) *The Playa 'Fault', evidence of a ductile shear zone and its relationship to gold mineralisation at the Revenge mine, Kambalda*. Unpublished WMC Technical Report No 006, SIGM Research Project K 521.

Nguyen, T. P., Powell, C. McA, Harris, L. B. and Hein, K. A. A. (1995) Development of vein systems in shear zones at Revenge mine, Kambalda, Western Australia: evidence of palaeoseismic events. In *Clare Valley International Conference, Specialist Group in Tectonics and Structure Geology, Geological Society of Australia Abstracts*, Vol. **40,** pp. 117–118.

Perring, C. S. (1988) Petrogensis of the lamprophyre "porphyry" suite from Kambalda, Western Australia. In *Recent Advances in Understanding Precambian Gold Deposits*, eds S. E. Ho and D. I. Groves, pp. 277–294. Geology Department and University Extension, The University of Western Australia Publication No 12.

Poulsen, K. H. and Robert, F. (1989) Shear zones and gold: practical examples from the Southern Canadian Shield. In *Mineralisation in Shear Zones*, ed. J. T. Bursnall, pp. 239–266. Geological Association of Canada Short Course Notes, **6**.

Ramsay, J. G. (1980) The crack-seal mechanism of rock deformation. *Nature* **284,** 135–139.

Robert, F. and Brown, A. C. (1986) Archaean gold-bearing quartz veins at Sigma mine, Abitibi greenstone Belt, Quebec: Part I, Geologic relations and formation of the vein system. *Economic Geology* **81,** 578–592.

Robert, F., Boullier, A. M. and Firdaous, K. (1995) Gold-quartz veins in metamorphic terranes and their bearing on the role of fluids in faulting. *Journal of Geophysical Research* **100,** 12,861–12,879.

Roberts, D. E. and Elias, M. (1990) Gold Deposits of the Kambalda–St Ives Region. In *Geology of the Mineral Deposits of Australia and Papua New Guinea*, ed. F. E. Hughes. The Australasian Institute of Mining and Metallurgy, Melbourne.

Secor, D. T. (1965) Role of fluid pressure in jointing. *American Journal of Science* **263,** 633–646.

Sibson, R. H. (1981) Fluid flow accompanying faulting: Field evidence and models. In *Earthquake prediction: An international review*, eds D. W. Simpson and P. G. Richards, pp. 593–603. American Geophysical Union, Maurice Ewing Series, **4**.

Sibson, R. H. (1985) A note on fault reactivation. *Journal of Structural Geology* **7,** 751–754.

Sibson, R. H. (1989) Earthquake faulting as a structural process. *Journal of Structural Geology* **11,** 1–14.

Sibson, R. H. (1990) Faulting and fluid flow. In *Fluids in Tectonically Active Regimes of the Continental Crust*, ed. B. E. Nesbitt, pp. 93–132. Mineralogical Association of Canada, Short Course Handbook, **18**.

Sibson, R. H. (1992) Implications of fault-valve behaviour for rupture nucleation and recurrence. *Tectonophysics* **211,** 283–293.

Sibson, R. H. (1993) Load-strengthening versus load-weakening faulting. *Journal of Structural Geology* **15,** 123–128.

Sibson, R. H., Robert, F. and Poulsen, K. H. (1988) High-angle reverse faults, fluid pressure cycling and mesothermal gold–quartz deposits. *Geology* **16,** 551–555.

Suppe, J. (1985) *Principles of Structural Geology*. Prentice Hall, Englewood Cliffs, N.J.

Swager, C. P. (1989) Structures of the Kalgoorlie greenstones—regional deformation history and implications for the structural setting of gold deposits within the Golden Mile. *Geological Survey of Western Australia, Report* **25,** 59–84.

Swager, C. P. (1991) *Geology of the Menzies 1:100,000 Sheet*. Geological Survey of Western Australia, Record, p. 1990/4.

Swager, C. P., Witt, W. K. and Griffin, T. J. (1990a) A regional overview of the Late Archaean Kalgoorlie granite–greenstones of the Kalgoorlie Terrane. In *Third Archaean International Symposium, Perth, 1990, Excursion Guidebook*, eds S. E. Ho, J. E. Glover, J. S. Myers and J. R. Muhling, pp. 205–220. Geology Department and University Extension, The University of Western Australia Publication, **21**.

Swager, C. P., Witt, W. K., Griffin, T. J., Ahmat, A. L., Hunter, W. M., McGoldrick, P. J. and Wyche, S. (1990b) Late Archaean granite–greenstones of the Kalgoorlie Terrane, Yilgarn Craton, Western Australia. In *Third International Archaean Symposium, Perth, 1990, Proceedings volume*, eds J. E. Glover and Se Ho, pp. 107–122. Geology Department and University Extension, University of Western Australia Publication, **22**.

Vearncombe, J. R. (1993) Quartz vein morphology and implications for formation depth and classification of Archaean gold-vein deposits. *Ore Geology Reviews* **8,** 407–424.

Witt, W. K. (1990) *Geology of the Bardoc 1:100,000 Sheet*. Geological Survey of Western Australia, Record, p. 1990/14.

Wong, T. (1986) Metamorphic patterns in the Kambalda area and their significance to Archaean greenstone belts of the Kambalda–Widgiemooltha area. Unpublished BSc (Honours) thesis. The University of Western Australia.

Woodall, R. (1990) Gold in Australia. In *Geology of the Mineral Deposits of Australia and Papua New Guinea*, ed. F. E. Hughes, pp. 45–67. Australasian Institute of Mining and Metallurgy, Melbourne.